LUND UNIVERSITY
Faculty of Science

Planetary boundary layer height measurements in a rural environment in southern Sweden

Relation to meteorological parameters and aerosol particle concentrations

Ellen Carneheim

Thesis submitted for the degree of Bachelor of Science
Project duration: 4 Months

Supervised by Adam Kristensson, Thomas Bjerring Kristensen, and Erik Thomsson

Department of Physics
Division of Nuclear Physics
May, 2020

Abstract

The aim of this project is to analyse planetary boundary layer height (BLH) measurements from the Hyltemossa research station and find their dependence on seasonality, time of day, and air temperature. Further, investigation was made into the correlation between mass concentration of particulate matter with equivalent diameter $< 1\mu$m (PM_1) and black carbon (BC) aerosol and the BLH and how this varies between seasons and wind directions. Measurements of BLH were made using a VAISALA CL51 ceilometer. It was found that there is a clear diurnal variation of BLH in all seasons but winter and that the BLH is dependent on temperature in summer. Moreover, anti-correlation between BLH and both BC and PM_1 were found in winter and fall and the correlation with PM_1 was stronger when southerly winds prevailed than when northerly winds prevailed.

Contents

Acronyms

BLH	Boundary Layer Height
PBL	Planetary Boundary Layer
ML	Mixed Layer
BC	Black Carbon
PM_1	Particulate Matter with equivalent diameter $< 1\mu$m
PM_{10}	Particulate Matter with equivalent diameter $< 10\mu$m
ACTRIS	Aerosol, Clouds and Trace Gases Research Infrastructure
ICOS	Integrated Carbon Observation System
BVOCs	Biogenic Volatile Organic Compounds
SW	Southwest
SE	Southeast
NW	Northwest
NE	Northeast

1 Introduction

Air pollution has a big impact on human health and climate and is therefore of interest for many studies around the world. One of these is the Aerosol, Clouds and Trace Gases Research Infrastructure (ACTRIS), a pan-European initiative comprising of several atmospheric field stations for the research in that area (ACTRIS, 2015). At the Hyltemossa Research station in northern Scania (Sweden), ACTRIS has a cooperation with the Integrated Carbon Observation System (ICOS) for research on the uptake and release of greenhouse gases from various ecosystems including measurements of aerosol concentrations, air temperature, wind speed, and wind direction (ICOS-Sweden, 2018).

It is known that meteorological parameters such as wind, humidity and Boundary Layer Height (BLH) can affect the aerosol concentration in the atmosphere (Mues et al., 2017). Therefore, this connection should be further researched at the Hyltemossa station. Since June 2017, a VAISALA CL51 Ceilometer has been measuring the backscatter from the atmosphere at the Hyltemossa station to deduce the BLH and cloud base height. The aim of this study is to analyse the BLH celiometer data and it's dependence on seasonality, time of day, and temperature. Moreover, it is investigated how the mass concentration of particulate matter with equivalent diameter $< 1\mu$m (PM_1) and Black Carbon (BC) are affected by the BLH and how this correlation is affected by seasonality and wind direction.

2 Background

2.1 Planetary Boundary Layer

The Planetary Boundary Layer (PBL) is the lowest layer of the atmosphere which is directly influenced by the Earth's surface and responds to forcings thereof in less than an hour. These forcings can be frictional drag, thermal processes caused by radiation, evaporation, and condensation, pollutant emissions and flow alterations caused by topography. The PBL height (BLH) is the height of the top of this layer where there is often a strong temperature inversion, separating the PBL from the free atmosphere above. This height varies significantly depending on time of day, season, location, and weather and is usually 50-3000 meters above the surface. The BLH is often much higher in a low pressure region than in a high pressure region. Within the PBL turbulence is of big importance since this mixes the air (Stull, 1988).

2.2 Diurnal Variation and Structure of the PBL

The PBL has a clear diurnal variation and in high pressure regions it has a clear structure, while the structure is less defined in low pressure areas (Stull, 1988). Air does not readily absorb the wavelengths of solar radiation (0.3 μm-1.0 μm), so when the sun rises, most of its energy passes through the atmosphere to the ground. The ground is then heated and this heat is transferred to the air molecules closest to the surface through conduction. However, since air is a bad conductor of heat this only affects the few centimeters closest to the surface. This air is now less dense than the air above causing convection and rising of the BLH. The upward moving air creates thermal turbulence since the rising air acts as an obstacle for the winds creating eddies in the wind flow. Moreover, the exchange of air with the stronger winds aloft strengthens winds at the surface, which results in more mechanical turbulence due to obstacles on the ground. Within the PBL there are many eddies of different sizes referred to as turbulence (Ahrens & Henson, 2016). This unstable layer is then present throughout the day reaching its maximum depth in the afternoon. Due to the turbulence, heat, moisture, momentum, and aerosols are well mixed within this layer and it is therefore called the Mixed Layer (ML). Around sunset, the heating of the ground is no longer sufficient to fuel the convection, so turbulence decreases. Moreover, the cooling of the surface creates a stable (nocturnal) boundary layer that grows deeper until sunrise. Above this stable layer, a so called residual layer is formed where turbulence is uniform in all directions and the initial state is the same as in the ML that was present the day before (Stull, 1988). The homogeneous dispersion of pollutants in the height is of great importance to air quality since it can decrease the aerosol concentration within it (Mues et al., 2017).

2.3 Aerosol

An aerosol is a group of solid or liquid particles suspended in a gas long enough to be observed or measured. To be able to compare particles of different shape, a so called equivalent diameter is calculated for each particle. How this is calculated depends on what property of the particles are of interest. In many cases this is the aerodynamic equivalent diameter which is the diameter of a spherical particle of standard density (1000 kg/m^3) which has the same gravitational settling velocity as the particle being measured. Aerosols are often divided into groups according to their size, for example PM_1 and PM_{10} (particulate matter with equivalent diameter $< 1\mu$m and $< 10\mu$m respectively). The size of the particle is of importance because this

can determine the effect it has on human health and climate. For this, the chemical composition of the particle is also relevant (Kulkarni et al., 2011). BC is particulate matter, mostly in the sub-micrometre diameter range, consisting of pure carbon which is formed through incomplete combustion of biomass, fossil fuels, and bio fuels (Martinsson et al., 2017). There are different types of measurements of aerosol concentration, one of these is mass concentration which is the mass of all particulate matter in a certain volume of gas, normally in units of $\mu g/m^3$ (Kulkarni et al., 2011).

2.4 Sources of Aerosols

There are two different types of particles, primary particles and secondary particles. The former can be mechanically generated by for example wind blown dust or road abrasion, or formed from combustion of for example biomass or fossil fuels. They can also originate from volcanoes and biological sources such as pollen. The latter, secondary particles, are formed by condensation on already existing particles or by creation of new particles from gaseous precursors (Kristensson, 2005). One example of this is the nucleation or condensation of Biogenic Volatile Organic Compounds (BVOCs), which is released by plants and trees mostly during warm and dry seasons (Oderbolz et al., 2013). Aerosol concentrations at any location can depend both on local sources and transport in different layers of the atmosphere. Aerosols brought by winds from a highly polluted area can then be transported through the inversion layer into the PBL and vice versa (Miao et al., 2018).

3 Method

3.1 Hyltemossa Site Description

The Hyltemossa research station is located south of Perstorp in northern Scania in southern Sweden (56°06′N, 13°25′E, 115 m asl) and belongs to the ICOS and ACTRIS networks. The site is in the middle of a 30 year old spruce forest, dominated by Norwegian spruce as seen in figure 1, located far from any major towns and roads. All meteorological measurements are made in a 150 meter high tower and aerosol measurements are made in a 30 meter high tower on top of a lab house in a small clearing in the trees, seen in figure 2 (ICOS-Sweden, 2018). The ceilometer is placed on the roof of the lab house, marked with a green ellipse in figure 2.

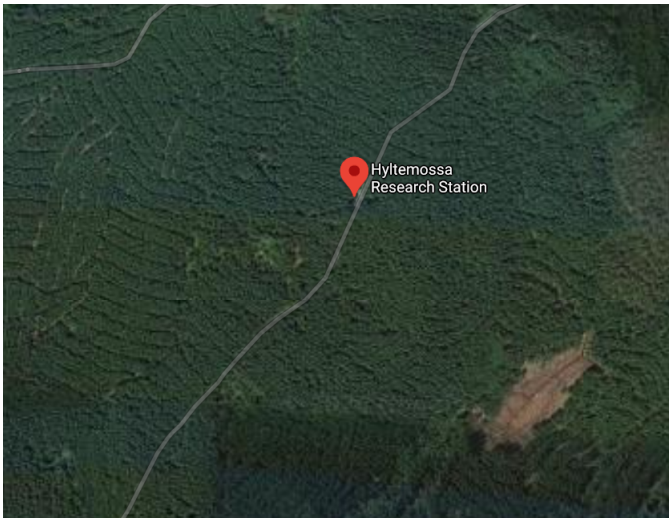

Figure 1: *Satellite image of the Hyltemossa Research station with surroundings (Google-Maps, 2020).*

Figure 2: *Aerosol measuring tower and the roof of the lab house at Hyltemossa research station. The green ellipse marks the ceilometer. The 150 m tower is located behind the photographer.*

3.2 Hallahus Site Description

The Hallahus measurement station is located near Klåveröd (56°02'32.7"N 13°08'54.4"E) about 25 km from Hyltemossa, also far from any major towns or roads, as seen in figure 3. Figure 4 shows that the station is placed on a grass field, about 100 m wide, surrounded by forest.

Figure 3: *Satellite image showing the location of the Hyltemossa research station and Hallahus measuring station (Google-Maps, 2020).*

Figure 4: *Satellite image of the Hallahus measuring station with surroundings (Google-Maps, 2020).*

3.3 VAISALA CL51 Ceilometer

A ceilometer is an instrument that measures the backscatter (reflection of light) from obstacles vertically in the atmosphere using light detection and ranging (LIDAR) technology, so that different atmospheric parameters, such as cloud base height, boundary layer height, and visibility can be calculated. Once every 16 seconds it sends a diode laser pulse with wavelength 910 nm in a vertical or near-vertical direction. The backscatter from obstacles in the atmosphere, such as cloud droplets or aerosol particles, are then detected with a resolution of 10 meters and analyzed by the instrument to make a vertical backscatter profile of up to 15 km, calculate the height of three cloud layers up to 13 km and the BLH (VAISALA, 2018). To find the boundary layer height, the gradient method is used. In this method, it is assumed that aerosols are evenly distributed in the PBL and that there is a large decrease in aerosols in the inversion layer. Therefore, the boundary layer height is calculated by finding local gradient minima in backscatter from aerosols. Other minima could be found and can indicate other layers in the atmosphere, such as the residual layer or other elevated aerosol layers (Münkel & Roininen, 2007). Clouds give a much stronger backscatter signal, so, the cloud base height is determined by finding areas with higher response (Lotteraner & Piringer, 2016). The measurements used in this project are from the 21^{st} of June 2017 to 31^{st} of December 2019.

3.4 Aerosol Measurements

3.4.1 Palas FIDAS 200 S

The PM_1 and PM_{10} concentration measurements were made with a Palas aerosol spectrometer of model FIDAS 200 S. It does this by drawing in ambient air through a Sigma 2 sampling head and an Intelligent Aerosol Drying System (IADS), preventing condensation which could cause measurement errors, with a total flow rate of 4.62 l/min. This system is regulated by measurements of air temperature, pressure, and humidity provided from a weather station included in the instrument set-up. The air then moves through a chamber which is homogeneously illuminated by white light using a polychromatic LED light output. Each particle will then cause Lorenz-Mie scattering which a sensor detects at an angle of 85-95°. The number of scattered pulses determines the amount of particles measured and the intensity of the scatter signal gives the size of each particle so that the hourly PM_1 and PM_{10} concentrations can be calculated. The instrument is calibrated using a monodisperse test aerosol (Palas, 2015). The measurements used in this project are from 9^{th} of May 2018 to 16^{th} of December 2019.

3.4.2 Aethalometer AE33

BC aerosol concentration measurements were made with a Magee-Scientific Aethalometer model AE33. Air is continuously drawn in through a Thermo fisher PM-10 USEPA inlet at the height of 30 m with a total flow rate of 16.7 l/min and continues down to the lab house where the flow is divided to different instruments with a flow of 5 l/min to the aethalometer. There, it is drawn through a spot on a filter tape, model PN 8060 (Aerosol d.o.o., Ljubljana, Slovenia), so that aerosol particles accumulate in that spot. Two filter tapes with different rates of accumulation were used to correct errors due to filter loading. BC concentration measurements per minute were made using light absorption coefficients from seven wavelengths between 370-950 nm by illuminating the tapes (Magee-Scientific, 2018). All default settings recommended by the manufacturer were used. The measurements used in this project are from the 1^{st} of January to the 18^{th} of November 2019.

3.5 Meteorological Measurements

Meteorological measurements of air temperature, wind direction and wind speed were made and controlled by ICOS Sweden using different instruments installed at the 70 m height in the measurement tower (ICOS-Sweden, 2018). Air temperature was measured using a Rotronic MP102H sensor with a HC2A-S3 hygroclip covered by a passive ventilated radiation shield (Rotronic, n.d.). The data was then logged in a Campbell Scientific CR1000X logger (Campbell-Scientific, 2017). Wind speed and direction were measured using a Metek uSonic-3 anemometer (METEK, n.d.). The measurements used in this project are from the 26^{th} of September 2017 to 31^{st} of December 2019.

3.6 Data Processing

All data was divided according to the seasons in which it was measured with winter consisting of December, January, and February, spring consisting of March, April, and May, summer consisting of June, July, and August, and fall consisting of September, October, and November. Measurements of BLH higher than 3000 m or lower than 50 m were excluded, since this is the range of BLH stated in the PBL theory (see section 2.1). The 25^{th}, 50^{th}, and 75^{th} percentile of BLH was calculated for each hour of the day for each season of each year and the average temperature was calculated for all of these. The median of the BLH was calculated for every hour of measurements excluding error measurements and these were compared to measures of mean temper-

ature for those hours by calculating the mean measurement of temperature and standard deviation in 250 m bins of BLH. Correlation coefficients and p-values were calculated for mean temperature and BLH for each season, where the correlation coefficient is a measure of the strength of connection between the relative movements of two variables where -1 means absolute anti-correlation, 1 means perfect correlation, and 0 means no correlation, and the p-value is a measure of the statistical significance of the correlation coefficient where p-values < 0.05 shows significant correlation (Weinberg & Schumaker, 1962).

The median of BC concentration measurements was calculated for each hour. The PM_1 and BC concentration measurements were compared with the hourly data of BLH and divided into 250 m bins of BLH and then plotted in a box plot where the 0^{th}, 25^{th}, 50^{th}, 75^{th}, and 100^{th} percentiles are shown and the number of measurements in each bin was recorded. This was done with all data and for each season. Further, the data was divided into sectors of wind direction where Northeast (NE) is from 0° to 90°, Southeast (SE) is from 90° to 180°, Southwest (SW) is from 180° to 270°, and Northwest (NW) is from 270° to 360°, and box plots were made for these as well. Correlation coefficients and p-values were calculated for each season and wind direction. Moreover, the median PM_1 and BC concentration were calculated for 10° bins of wind direction for all available data and for winter and summer measurements separately. The median PM_1 and BC concentration was calculated for each hour of the day in winter and summer.

4 Results and Discussion

4.1 Diurnal Variation of BLH and Temperature Dependence

Figure 5 shows the diurnal variation of the BLH for the different seasons and years as it shows the median and the 25^{th} and 75^{th} percentile for all measurements made each hour of the day. From this figure, it can be seen that there is a clear diurnal variation of the BLH in spring, summer, and fall with a maximum height some time in the afternoon and a minimum height during the night or early morning as was described in section 2.2. However, this is not the case for winter where the BLH only has small variations throughout the day. The reason for this could be the variation in solar radiation between the seasons; it is lowest in the winter and highest in the summer. As described in the background, heating of the surface is needed

for the BLH to grow during the day which is greatly dependent on the solar radiation. From figure 5, it seems that the solar radiation is sufficient to fuel the lifting of the BLH in all seasons but winter at the Hyltemossa station. Global radiation measurements at the top of the 150 m tower confirm the seasonal variability of radiation at Hyltemossa.

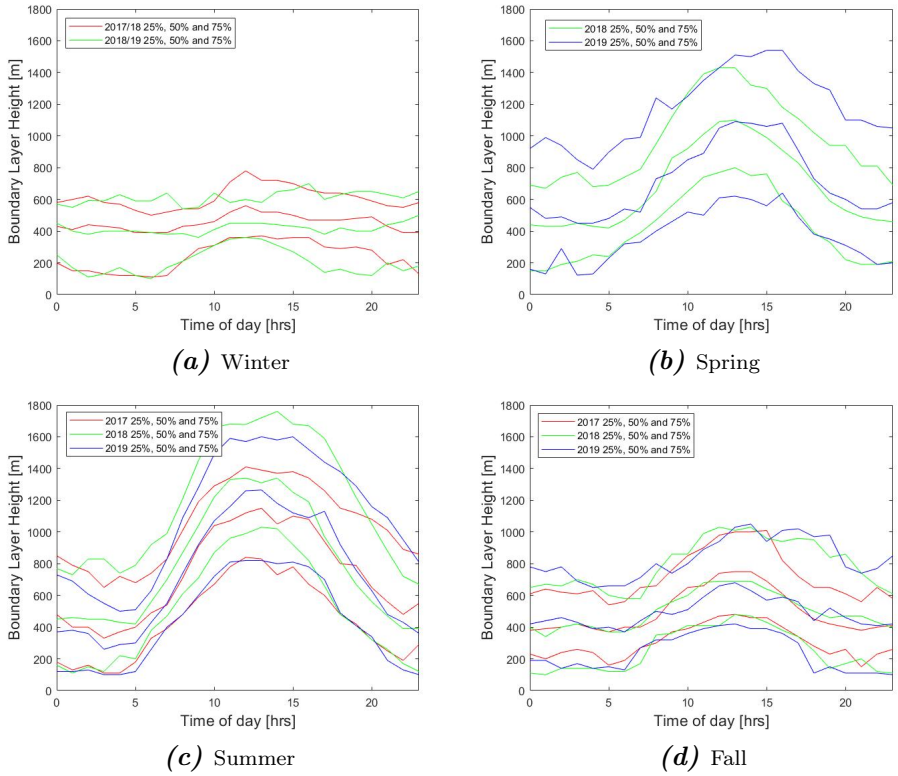

(a) Winter ***(b)*** Spring

(c) Summer ***(d)*** Fall

Figure 5: *This figure shows the diurnal variation of the BLH for a) winter, b) spring, c) summer, and d) fall, each separated into the years where data was available. The three lines for each year represents the* 25^{th}*,* 50^{th} *and* 75^{th} *percentile.*

Comparing the diurnal variation of BLH for different years for all seasons in figure 5, it can be seen that the differences between the years are not significant in winter, spring, and fall. However, the measurements of BLH for summer 2018 are prominently higher during the daytime hours than summer 2017 and 2019 for all shown percentiles. Table 1 shows the mean temperature of all seasons with available data from ICOS. Here it is seen that there is a considerable difference in mean temperature between summer 2018 and 2019. This is probably the reason for the difference in BLH between the years since figure 6 and the correlation coefficient and p-value for summer in table 2 show a clear correlation between temperature and BLH in summer. Even

though the difference in mean temperature between the years is significant for the other seasons as well, the difference in BLH is not as clear as for the summer measurements. This is probably because the correlation between BLH and temperature, shown in figure 6 and by the correlation coefficients and p-values in table 2, is not as strong for the other seasons.

Table 1: *Mean temperature of each season and year.*

Season	Year	Mean Temperature (°C)
Spring	2018	7.52
	2019	7.11
Summer	2018	18.04
	2019	16.93
Fall	2017	7.43
	2018	9.25
	2019	8.67
Winter	2017-2018	0.43
	2018-2019	1.88

Table 2: *Calculated correlation coefficients and p-values between temperature and BLH for each season. Significant correlation coefficients (> 0.25) with p-values < 0.05 are marked with bold text.*

Season	Correlation Coefficient	p-value
Winter	-0.06	0.0299
Spring	0.23	$4.25 \cdot 10^{-30}$
Summer	**0.48**	$3.90 \cdot 10^{-218}$
Fall	**0.25**	$6.39 \cdot 10^{-48}$

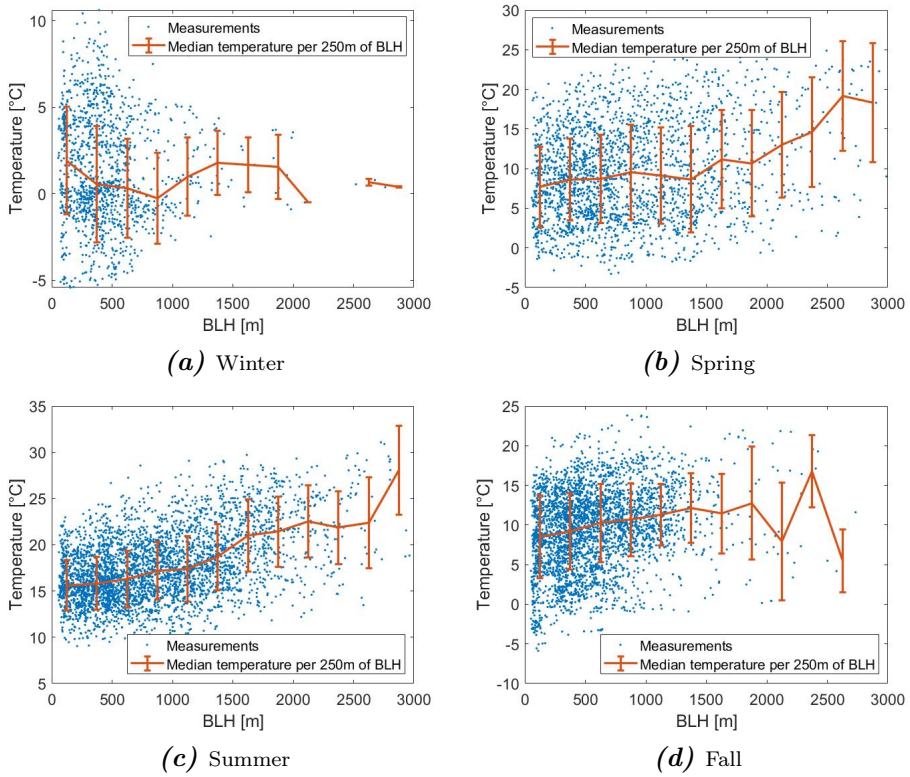

(a) Winter *(b)* Spring

(c) Summer *(d)* Fall

Figure 6: *Scatter plot of measurements of temperature and BLH with red graph showing the mean of 250 m bins of BLH with standard deviation variability bars for a) Winter, b) Spring, c) Summer, and d) Fall.*

4.2 BLH and Aerosol Concentration

4.2.1 PM_1

Figure 7a indicates that there should be some interrelationship between BLH and PM_1 concentration for BLH lower than 1500 m since the PM_1 concentration decreases as the BLH increases for all percentiles in the 250 m bins. However, the correlation coefficient between these two variables for all measurements seen in table 3 shows that the correlation is not very strong. This is probably because there is a big variation in BLH between the seasons, as shown in section 4.1. Moreover, figure 8 shows that the PM_1 concentration is dependent on wind direction. Because of the differences between the seasons and wind directions, there is probably too much variation in the data to get a clear result.

Figure 8 shows that air coming from the SE mostly has a much higher PM_1

concentration than other wind directions. These air masses are often coming from Poland and other eastern European countries that are relatively more polluted than other areas. This pollution could be carried by the wind to Hyltemossa. Although there are areas with high pollution SW of Scania in western Europe, these air masses are probably cleaner because they are often associated with low pressure systems with comparably more precipitation and high wind speeds mixing the air, while air masses from the SE more often are paired with high pressure systems with more dry weather. Moreover, air masses from the south are usually warmer which could act as a lid prohibiting the growth of the BLH and therefore cause less spread of aerosols as suggested by Miao et al. (2018) in a study in China. Air masses coming from NE and NW are probably cleaner due to less pollution in the Nordic countries. This result was also found for the particle number size distribution by Kristensson et al. (2008) by trajectory analysis for the Vavihill measurement station close to Hyltemossa. These meteorological systems can partly be seen in a study by Esteban et al. (2006) where long term flow patterns over western Europe were studied.

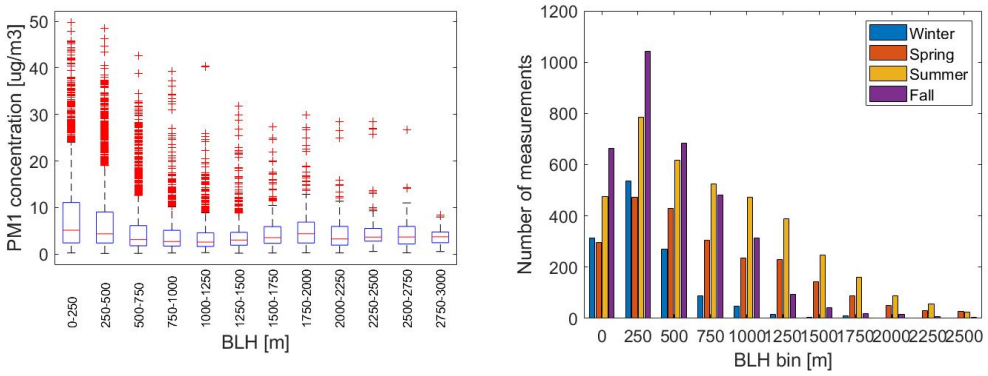

Figure 7: *a) Box plot of all PM_1 measurements in 250m bins where the red lines mark the median, the blue boxes show the 25^{th} and 75^{th} percentile, the dashed lines show the 0^{th} and 100^{th} percentile, and the red crosses show the outliers. b) Number of measurements in each bin for each season*

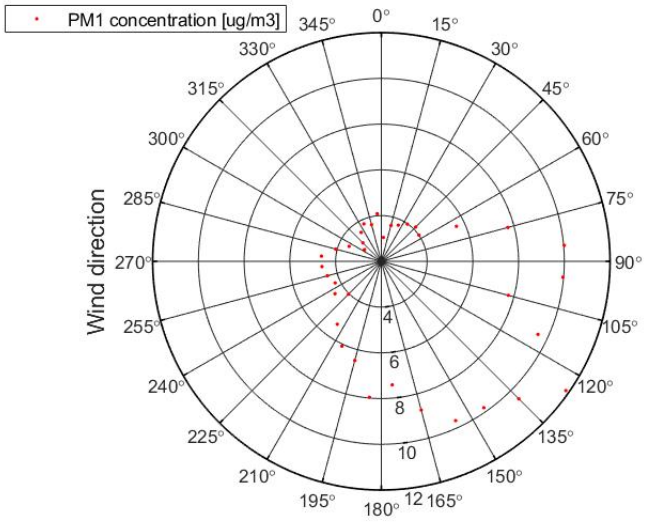

Figure 8: *Polar plot showing median PM1 concentration for measurements within a 10 ° bin of wind direction where the radius is the PM1 concentration and the angle is the wind direction.*

Table 3: *Correlation ceofficients and p-values for correlation between BLH and PM_1 concentration for the different seasons and wind directions where stronger anti-correlations (< -0.25) are marked with bold text.*

Season	Wind direction	Correlation Coefficient	p-value
All	All	-0.19	$2.28 \cdot 10^{-87}$
	NW	-0.11	$7.18 \cdot 10^{-10}$
	NE	-0.04	0.08
	SW	**-0.26**	$7.16 \cdot 10^{-56}$
	SE	**-0.30**	$3.51 \cdot 10^{-53}$
Winter	All	**-0.27**	$8.05 \cdot 10^{-23}$
	NW	-0.24	$2.45 \cdot 10^{-7}$
	NE	-0.23	$6.28 \cdot 10^{-4}$
	SW	**-0.32**	$1.11 \cdot 10^{-10}$
	SE	**-0.27**	$2.69 \cdot 10^{-5}$
Spring	All	-0.11	$3.11 \cdot 10^{-7}$
	NW	-0.06	0.124
	NE	-0.22	$1.39 \cdot 10^{-7}$
	SW	-0.13	$3.30 \cdot 10^{-3}$
	SE	-0.19	$4.46 \cdot 10^{-6}$
Summer	All	-0.09	$5.07 \cdot 10^{-9}$
	NW	-0.07	$1.56 \cdot 10^{-2}$
	NE	-0.15	$2.10 \cdot 10^{-3}$
	SW	-0.17	$6.31 \cdot 10^{-10}$
	SE	-0.05	0.127
Fall	All	**-0.31**	$5.32 \cdot 10^{-76}$
	NW	-0.17	$2.95 \cdot 10^{-5}$
	NE	-0.13	$1.90 \cdot 10^{-3}$
	SW	**-0.34**	$7.70 \cdot 10^{-38}$
	SE	**-0.29**	$3.63 \cdot 10^{-17}$

The correlation coefficients in table 3 show that the anti-correlation is much stronger between PM_1 concentration and BLH for measurements with wind direction SE or SW than for NE and NW, which is also seen in figure 9d, and partly in 9c, where all percentiles of PM_1 concentration decrease with height. This is probably because of the meteorological differences between the wind directions. Low pressure areas, often coming to Scania from west or north, bring fronts with strong winds and precipitation, while high pressure areas, often coming from the south or east, bring more clear weather as described by Ahrens and Henson (2016). Winds and precipitation have a big impact on aerosol concentrations since winds can bring more aerosols to

the air by lifting dust and precipitation brings aerosols out of the air to the ground. This could mean that the BLH is of less importance for the PM_1 concentration when many low pressure areas are passing since there are so many other meteorological factors affecting it. In high pressure areas there are not as many other meteorological factors than the mixing of air in the PBL affecting the PM_1 concentration. This is probably why the correlation between PM_1 and BLH is much stronger when the wind is coming from the SE.

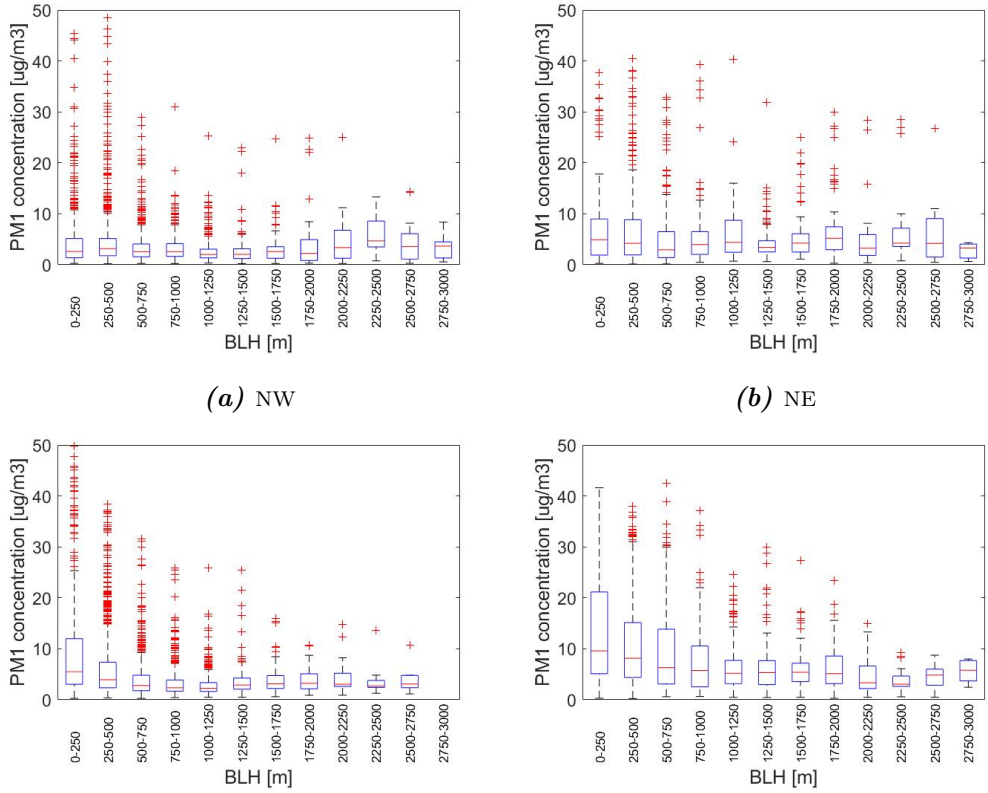

(a) NW ***(b)*** NE

(c) SW ***(d)*** SE

Figure 9: *Boxplot for PM1 concentrations in 250 m bins of BLH where the red lines mark the median, the blue boxes show the 25^{th} and 75^{th} percentile, the dashed lines show the 0^{th} and 100^{th} percentile, and the red crosses show the outliers for wind direction sectors a) NW, b) NE c) SW, and d) SE*

Figure 10 shows that there are high concentrations of PM_1 from many wind directions in summer while the concentrations are much higher with winds from the SE in Winter. This could be because biogenic sources of PM_1 are much more prominent than anthropogenic ones in summer, while the situation is opposite in the winter, as found by Genberg et al. (2011). Biogenic

sources are more active in summer with particles from for example pollen and oxidation of certain types of BVOCs. Moreover, Fors et al. (2011) found that the secondary hygroscopic growth of particles is stronger in the summer aided by the increase of BVOCs produced. The biogenic sources of aerosols are not more prominent in any particular direction from Hyltemossa which means that the PM_1 concentration is not as dependent on wind direction. In winter, the wind direction is of more importance due to the larger source of particles from SE and the meteorological differences as discussed in the previous paragraph.

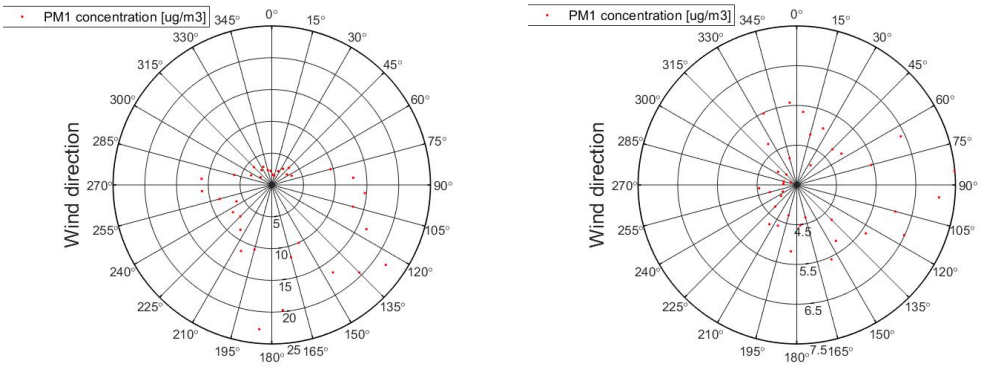

(a) Winter ***(b)*** Summer

Figure 10: *Polar plots of mean PM_1 concentration for 10º wind direction where the radius represent the PM_1 concentration and the angle the wind direction for a) winter and b) summer.*

The correlation coefficients in table 3 show an anti-correlation between PM_1 concentration and BLH for winter and fall but a weaker correlation for spring and summer. This can also be seen in figure 11 if measurements above 1500 m are dismissed, which could be motivated by figure 7b that shows that there are very few measurements above that height for all seasons, especially winter. The reason for the seasonal difference could be the variation of aerosol sources between seasons as discussed in the previous paragraph. Figure 7b shows that most measurements of BLH in the winter are below 700 m, which the very small diurnal variation shown in figure 5a also indicates. This means that the height in which the large amount of locally sourced aerosols can disperse is usually not high, but on days with higher BLH the same amount of PM_1 can spread out through the whole height resulting in lower concentrations. In the summer, there is a clear diurnal variation of the BLH as seen in figure 5c which means that most of the measurements in the lower bins

shown in figure 11c are of the nocturnal boundary layer. Much of the aerosol that was in the PBL during the day is then in the residual boundary layer, so the concentration is not higher in the low nocturnal boundary layer than in the high ML during the day. A stronger correlation might be found if the height of the residual layer was used instead of the nocturnal boundary layer during the summer nights.

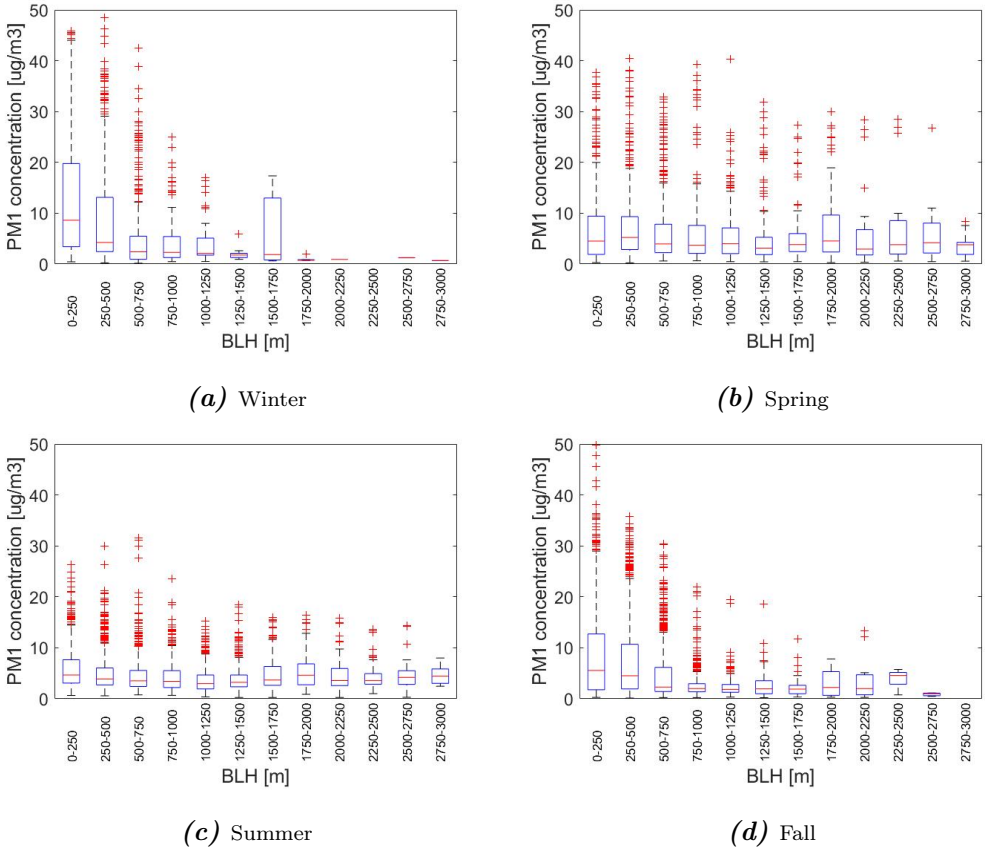

(a) Winter

(b) Spring

(c) Summer

(d) Fall

Figure 11: *Box plot of PM1 concentrations in 250m bins of BLH where the red lines mark the median, the blue boxes show the 25^{th} and 75^{th} percentile, the dashed lines show the 0^{th} and 100^{th} percentile, and the red crosses show the outliers for a) winter, b) Spring, c) summer, and d) fall.*

Figure 12 shows that there is some diurnal variation in PM_1 concentration for both winter and summer; however, the variation is much bigger in winter. The small variation of PM_1 concentration in summer indicates that the rising of the BLH during the day has some effect on the concentration. However, since the sources of aerosols are not local to as high an extent in summer as in winter, this effect is not extensive. The diurnal variation in winter is

probably not due to the BLH since the variation of that is not seen in this figure. It is more likely caused by domestic biomass combustion with a peak at night and a smaller peak in the morning since Genberg et al. (2011) found that this is a big source of aerosol in winter.

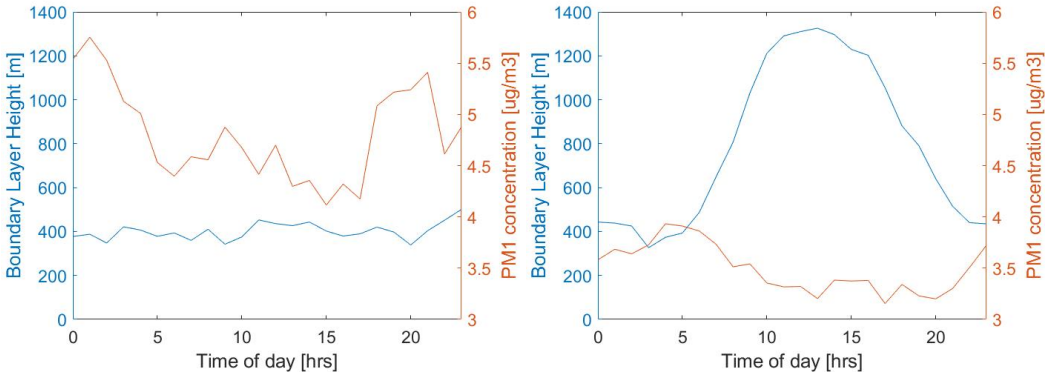

(a) Winter ***(b)*** Summer

Figure 12: *Diurnal variation of median BLH and PM_1 concentration for a) Winter and b) Summer.*

4.2.2 BC

The correlation between BC concentration and BLH seems to follow a similar pattern as the one for PM_1 as seen in figure 13a; however, the correlation coefficients for all seasons in table 4 and the number of outliers seen in figure 13a indicate that the correlation between the variables is not as strong as for PM_1. Figure 14 shows that the BC concentration is also dependent on wind direction, with much larger concentrations with winds coming from the SE. As with the PM_1 measurements, the anti-correlation between BC and BLH is stronger for southerly winds, as the correlation coefficients in table 4 show. However, in contrast to the PM_1 measurements, the correlation between BC concentration and BLH is not stronger for southerly winds than for northerly winds for each season individually. This is probably because there are much fewer measurements of BC then PM_1, as seen when comparing figure 13b and 7b.

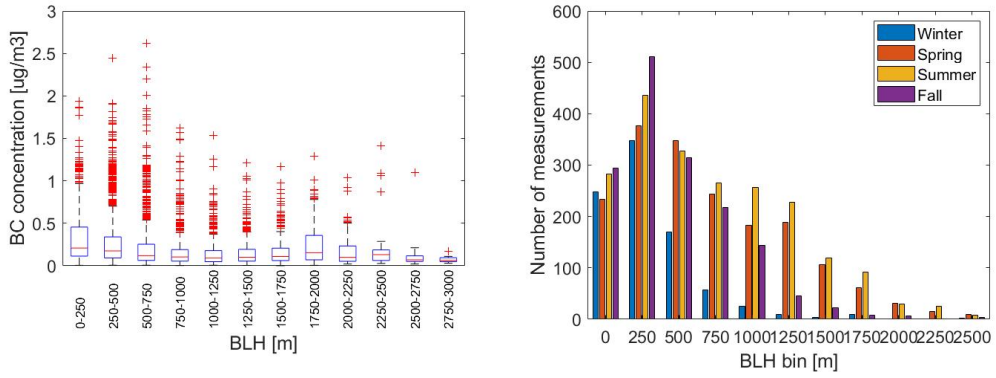

Figure 13: *a) Box plot of all BC concentration measurements in 250 m bins of BLH where the red lines mark the median, the blue boxes show the 25^{th} and 75^{th} percentile, the dashed lines show the 0^{th} and 100^{th} percentile, and the red crosses show the outliers. b) Number of BC measurements in each 250 m bin of BLH per season.*

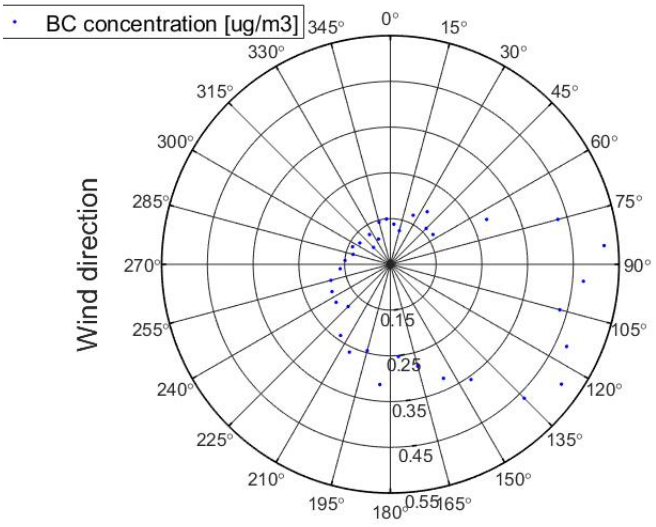

Figure 14: *Polar plot showing median BC concentration for measurements within a 10 ° bin of wind direction where the radius is the PM1 concentration and the angle is the wind direction.*

Table 4: *Calculated correlation coefficients and p-values for the correlation between BLH and BC concentration for the different seasons and wind directions. Significant correlation coefficinets (< -0.25) with p-values < 0.05 are marked with bold text.*

Season	Wind direction	Correlation Coefficient	P-value
All	All	-0.18	$5.16 \cdot 10^{-47}$
	NW	-0.18	$2.14 \cdot 10^{-15}$
	NE	-0.16	$2.09 \cdot 10^{-7}$
	SW	**-0.29**	$1.47 \cdot 10^{-43}$
	SE	-0.23	$5.40 \cdot 10^{-17}$
Winter	All	**-0.25**	$5.21 \cdot 10^{-14}$
	NW	**-0.29**	$1.35 \cdot 10^{-7}$
	NE	-0.21	0.045
	SW	**-0.34**	$5.13 \cdot 10^{-10}$
	SE	-0.21	$8.50 \cdot 10^{-3}$
Spring	All	-0.07	$3.40 \cdot 10^{-3}$
	NW	-0.08	0.05
	NE	-0.18	$3.09 \cdot 10^{-4}$
	SW	-0.09	0.05
	SE	-0.22	$2.34 \cdot 10^{-5}$
Summer	All	-0.07	$9.38 \cdot 10^{-4}$
	NW	-0.19	$1.23 \cdot 10^{-6}$
	NE	-0.14	0.03
	SW	-0.14	$2.11 \cdot 10^{-4}$
	SE	-0.09	0.03
Fall	All	-0.23	$9.37 \cdot 10^{-20}$
	NW	**-0.18**	$2.2 \cdot 10^{-3}$
	NE	-0.22	$2.15 \cdot 10^{-4}$
	SW	**-0.35**	$1.34 \cdot 10^{-19}$
	SE	-0.07	0.25

Figure 15 shows that the BC concentration is dependent on wind direction both in summer and in winter. This is probably because the BC is created through incomplete combustion which is mostly caused by anthropogenic activity. This means that the concentrations are higher from the SE during all seasons in the way that was discussed for PM_1 in section 4.2.1, which is a further indication that the sources of BC are from human activity even in summer, unlike with PM_1.

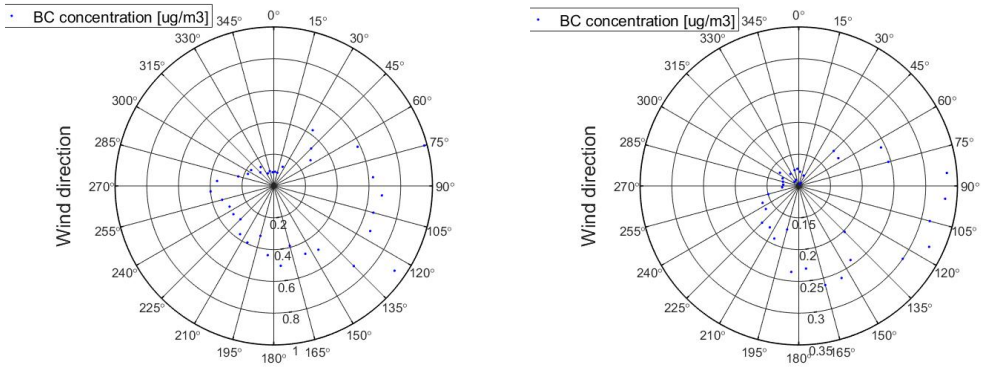

(a) Winter ***(b)*** Summer

Figure 15: *Polar plot showing median BC concentration for measurements within a 10 ° bin of wind direction where the radius is the PM1 concentration and the angle is the wind direction for a) Winter and b) Summer.*

As with the PM_1 values, the correlation coefficients shown in table 4 generally show a higher anti-correlation for fall and winter than for summer and spring which can also be seen in figure 16 if measurements above 1500 m are discarded. The reason for this is probably the same as for PM_1 as explained in section 4.2.1. The diurnal variation in winter seen in figure 17a, however, shows a much clearer pattern for BC concentration than PM_1. This is probably because all sources of BC are anthropogenic, so the diurnal pattern is because of human habits with high pollution from traffic and biomass burning during the awake hours so that the concentration is increasing throughout the day and then decreasing with lower activity during the night. The diurnal variation in summer is not clear as seen in figure 17b. A plausible reason for the similar BC concentrations for both night and day in summer is that during the day-light hours more traffic and other anthropogenic activities give higher emissions. At the same time, the BLH is higher meaning dispersion of the emissions vertically. During the night, the BLH is lower which gives less dispersion; however, there are less emissions, giving similar BC concentrations as during the day. Mues et al. (2017) found that in the Kathmandu valley, there was a clear diurnal pattern of BC concentrations with low concentrations during the day and high during the night for most seasons. The reason why the same results were not found in this study is probably the different meteorological conditions in Kathmandu compared to Hyltemossa. Moreover, the typography is very different so air mostly passes trough Hyltemossa from other areas with higher pollution while the valley in Kathmandu enables the local pollution to stay within the area. Moreover, many more measurements were excluded in that study such as those with

precipitation or fog, which was not done in the present study.

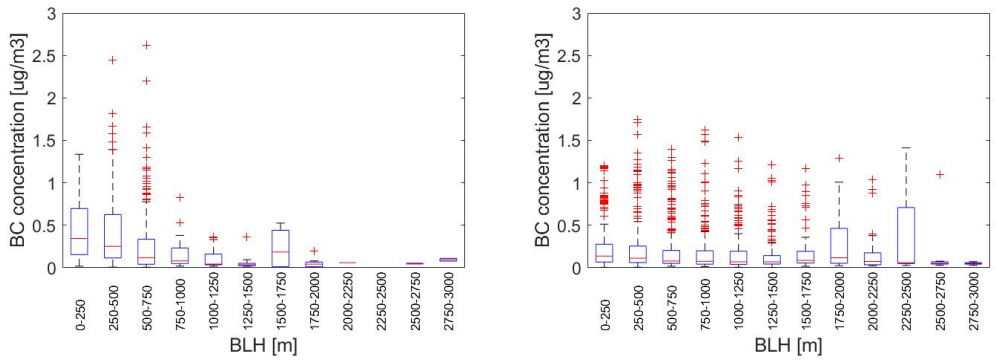

(a) Winter ***(b)*** Spring

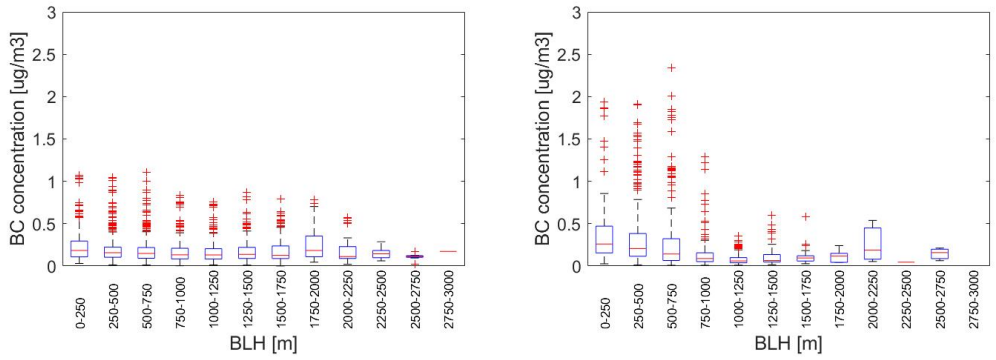

(c) Summer ***(d)*** Fall

Figure 16: *Boxplot of BC concentration in 250m bins of BLH where the red lines mark the median, the blue boxes show the 25^{th} and 75^{th} percentile, the dashed lines show the 0^{th} and 100^{th} percentile, and the red crosses show the outliers for a) Winter, b) Spring, c) Summer, and d) Fall.*

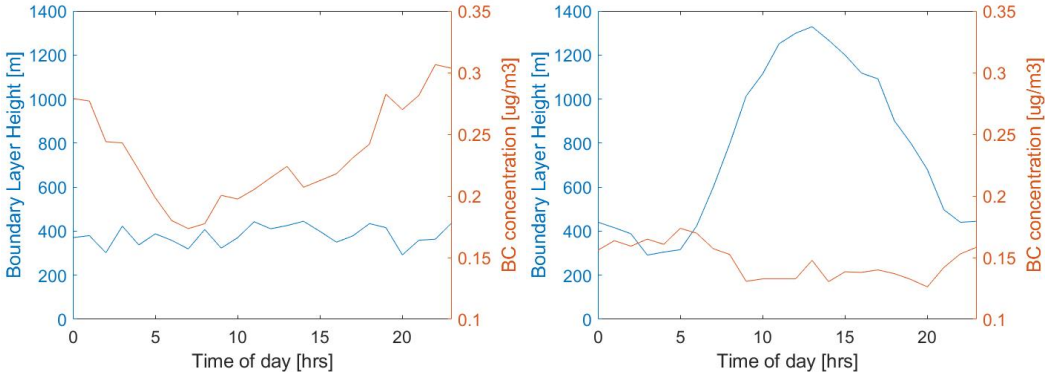

(a) Winter ***(b)*** Summer

Figure 17: *Median BLH and BC concentration for each hour of the day for a) Winter and b) Summer.*

In general, the anti-correlation seen between BLH and aerosol concentrations in this project is not very strong. This is probably because of the large spread of measurements within each bin seen in the box plots. This means that the anti-correlations found are just general tendencies of higher aerosol concentrations with lower BLH and vice versa, and not a general rule.

5 Conclusion

As expected, a clear diurnal variation of BLH was found for all seasons except for winter when the solar radiation is not strong enough to fuel the rise of the BLH during the day. In summer, a clear correlation between temperature and BLH gave an explanation for the higher BLH for each hour of the day in years with a higher mean temperature.

For both BC and PM_1 concentrations, some anti-correlation to the BLH was found. Concentrations of both types of aerosol were found to be dependent on wind direction, with higher concentrations with southeasterly winds. In summer, the sources of BC seem to be anthropogenic and therefore dependent on wind direction while PM_1 seem to originate from many different types of sources. In winter, concentrations of both types of aerosol are dependent on wind direction and therefore seem to be mainly anthropogenic. For PM_1 concentrations, higher anti-correlation to BLH was found with winds from the SE and SW than from the north; however, the anti-correlation was weaker for BC concentrations. Stronger anti-correlation between BLH and aerosol concentration was found for winter and fall than for summer and spring for both aerosol types.

6 Outlook

The results of this project are a small step towards understanding how the BLH affect the aerosol mass concentrations at the Hyltemossa research station, but much more could be done. In future studies, it should be investigated in which specific meteorological conditions the BLH plays the biggest role. This could be done by closer analysis on a day-to-day basis of meteorological, aerosol and BLH measurements instead of medians over a long period of time. Moreover, the sources of aerosol should be further investigated with the help of trajectory analysis and other source appointing methods, such as source/receptor modelling using trace elements in particles. A closer look at the backscatter profiles from the ceilometer, not available in this study, would also be of benefit for future projects to find when the BLH is a relevant factor influencing aerosol concentration levels.

Acknowledgements

First of all, I would like to thank my supervisor Adam Kristensson for his interest in and commitment to this project and the guidance and ideas he has given throughout this process. I would also like to thank Isabel Vinterbladh for vital help with programming in moments of need and frustration, and Jiři Navrátil for help with statistics and proof reading and general support this semester. I would also like to thank the co-supervisors in this project, Thomas Bjerring Kristensen and Erik Thomsson, and the staff at the Hyltemossa station for some help along the way. Lastly, I thank all my friends and family for their love and support.

References

ACTRIS. (2015). *Actris - a general description*. Retrieved April 28, 2020, from https://www.actris.eu/About/ACTRIS/WhatisACTRIS.aspx

Ahrens, G. D., & Henson, R. (2016). *Meteorology today - an introduction to weather, climate, and the environment* (11th ed.). Boston, Cengage Learning.

Campbell-Scientific. (2017). *Cr1000x - measurement and control datalogger*. Retrieved April 16, 2020, from https://www.campbellsci.com/cr1000x

Esteban, P., Martin-Vide, J., & Mases, M. (2006). Daily atmospheric circulation catalogue for western europe using multivariate techniques. *International Journal of Climatology*, *26*, 1501–1515.

Fors, E. O., Swietlicki, E., Svenningsson, B., Kristensson, A., Frank, G. P., & Sporre, M. (2011). Hygroscopic properties of the ambient aerosol in southern sweden – a two year study. *Atmospheric Chemistry and Physics*, *11*, 8343–8361.

Genberg, J., Hyder, M., Stenström, K., Bergström, R., Simpson, D., Fors, E. O., Jönsson, J. Å., & Swietlicki, E. (2011). Source apportionment of carbonaceous aerosol in southern sweden. *Atmospheric Chemistry and Physics*, *11*, 11387–11400.

Google-Maps. (2020). *Maps*. Retrieved April 17, 2020, from https://www.google.se/maps/@56.0832506,13.2357817,27990m/data=!3m1!1e3

ICOS-Sweden. (2018). *Hyltemossa*. Retrieved March 16, 2020, from https://www.icos-sweden.se/station_hyltemossa.html

Kristensson, A., Maso, M. D., Swietlicki, E., Hussein, T., Zhou, J., Kerminen, V.-M., & Kulmala, M. (2008). Characterization of new particle formation events at a background site in southern sweden: Relation to air mass history. *Tellus. Series B: Chemical and Physical Meteorology*, *60*(3), 330–344.

Kristensson, A. (2005). *Aerosol particle sources affecting the swedish air quality at urban and rural level* (Doctoral dissertation). Lund University. Lund.

Kulkarni, P., Baron, P. A., & Willeke, C. (2011). *Aerosol measurement - principles, techniques, and applications* (3rd ed.). Hoboken, John Wiley Sons.

Lotteraner, C., & Piringer, M. (2016). Mixing-height time series from operational ceilometer aerosol-layer heights. *Boundary-Layer Meteorology*, *161*, 265–287.

Magee-Scientific. (2018). *Magee scientific aethalometer model ae33*. Retrieved March 27, 2020, from https://mageesci.com/mproducts/model-ae33-aethalometer/

Martinsson, J., Azeem, H. A., Sporre, M. K., Bergström, R., Ahlberg, E., Öström, E., Kristensson, A., Swietlicki, E., & Stenström, K. E. (2017). Carbonaceous aerosol source apportionment using the aethalometer model – evaluation by radiocarbon and levoglucosa analysis at a rural background site in southern sweden. *Atmospheric Chemistry and Physics*, *17*, 4265–4281.

METEK. (n.d.). *Ultrasonic wind sensor usonic-3 omni*. Retrieved April 16, 2020, from https://metek.de/wp-content/uploads/2014/05/20150212_Datenblatt_uSonic3-Omni.pdf

Miao, Y., Guo, J., Liu, S., Zhao, C., Li, X., Zhang, G., Wei, W., & Ma, Y. (2018). Impacts of synoptic condition and planetary boundary layer structure on the trans-boundary aerosol transport from beijing-tianjin-hebei region to northeast china. *Atmospheric Environment*, *181*, 1–11.

Mues, A., Rupakheti, M., Münkel, C., Lauer, A., Bozem, H., Hoor, P., Butler, T., & Lawrence, M. G. (2017). Investigation of the mixing layer height derived from ceilometer measurements in the kathmandu valley and implications for local air quality. *Atmospheric Chemistry and Physics*, *17*(13), 8157–8176.

Münkel, C., & Roininen, R. (2007). *Mixing layer height assessment with a compact lidar ceilometer*. Retrieved March 9, 2020, from https://www.vaisala.com/sites/default/files/documents/Mixing_layer_height_assessment_with_a_compact_lidar_ceilometer.pdf

Oderbolz, D. C., Aksoyoglu, S., Keller, J., Barmpadimos, I., Steinbrecher, R., Skjøth, C. A., Plaß-Dülmer, C., & Prévôt, A. S. H. (2013). A comprehensive emission inventory of biogenic volatile organic compounds in europe: Improved seasonality and land-cover. *Atmospheric Chemistry and Physics*, *13*, 1689–1712.

Palas. (2015). *Fine dust measurement device fidas® 200 s*. Retrieved March 20, 2020, from https://www.palas.de/en/product/fidas200s

Rotronic. (n.d.). *Mp102h / mp402h*. Retrieved April 16, 2020, from https://www.rotronic.com/en/mp102h-mp402h.html

Stull, R. B. (1988). *An introduction to boundary layer meteorology*. Dordrecht, Kluwer Academic Publishers.

VAISALA. (2018). *Ceilometer cl51 for high-range cloud height detection*. Retrieved March 2, 2020, from https://www.vaisala.com/sites/default/files%20/documents/CL51-Datasheet-B210861EN.pdf

Weinberg, G. H., & Schumaker, J. A. (1962). *Statistics: An intuitive approach*. Belmont, Wadsworth Publishing Company.